

Correlations between Maximum Rate of Precipitation and Mesoscale Parameters

I. I. ZAWADZKI AND C. U. RO

Department de Physique, Université du Québec à Montréal, Québec, Canada H3C 3P8

(Manuscript received 15 November 1977, in final form 3 June 1978)

ABSTRACT

Daily 5, 10 and 30 min maxima of precipitation rate determined from a raingage network and radar were correlated with parcel convective energies, upper air humidity, height of parcel convection and maxima of surface conditions. After a selection of 54 well-documented cases the correlation coefficient between the maximum of rain rate over 5 min and the maximum convective energy was $\rho=0.79$ for all cases and $\rho=0.89$ for 15 air mass cases. Introducing the upper air humidity further improves the correlations.

1. Introduction

The statistical characteristics of precipitation have been studied by Huff and Ship (1969), Austin and Houze (1972) and Drufuca and Zawadzki (1975), to name just a few. Although very useful for practical applications, the statistical analysis of rain characteristics contributes little to the understanding of the precipitation process and leaves us with another descriptive picture of rain. The order, which is so hard to find in a precipitation pattern, is not found in the statistical domain. Some correlations between different precipitation parameters were investigated by Drufuca and Zawadzki (1975) and Drufuca (1977) with limited success. It appears that further efforts to describe the precipitation process by a limited number of parameters would require stratification of rain events into classes with differentiated characteristics. Mesoscale parameters associated with precipitation, if functionally related to the characteristics of rain, could provide the means for this stratification. The search for the relationships between mesoscale and rain parameters is the purpose of this work. The rain parameter chosen for this study is the maximum daily rainfall rate while the mesoscale parameters are the simple parcel convective energy and upper air humidity. Maximum rain rate correlates well with other statistical characteristics of rain (Drufuca and Zawadzki, 1975) and, in addition, it is the parameter which can be best related to simple parcel theory which applies reasonably well inside the protected core of the precipitating cell.

The idea of relating the parcel energy to the measured precipitation was used by Hamilton (1966) who found a close relationship between the height of the maximum radar echo and parcel energy. The urban thermal effect

was related to parcel energies by Harnack and Landsberg (1975) and others cited in their paper.

The present work is directed toward establishing a more quantitative and general relationship between precipitation and parcel energy. The data used in this study cover two summer seasons, May–September 1969–70. The data and the method used for the calculation of parcel energies are described in Section 2. Section 3 presents the correlations between maximum rain rates and maximum parcel energies. The effect of introducing the upper air humidity is discussed in Section 4. Some of the details needed for the proper evaluation of our results are given in Section 5, where an attempt is also made to answer some questions raised by the present work.

2. The data

Rain rate maxima over 5, 10 and 30 min were obtained from 14 tipping-bucket stations selected from the standard observational network of the Canadian Atmospheric Environment Service. The geographic distribution of the stations is shown in Fig. 1. There is a mean density of 1 gage every ~ 1500 km². In addition the entire region was routinely scanned by the McGill weather radar, giving a complete pattern of precipitation every 5 min. For the period analyzed the radar data were quantized in steps of 10 dB and were thus not adequate for a quantitative study of the nature intended here. Accordingly, they were used qualitatively in support of the gage network. The Canadian Atmospheric Environment Service provides an analysis of the raingage data, part of which are the rain rate maxima taken over 5, 10 and 30 min for every 24 h period used in this study. The times of occurrence of

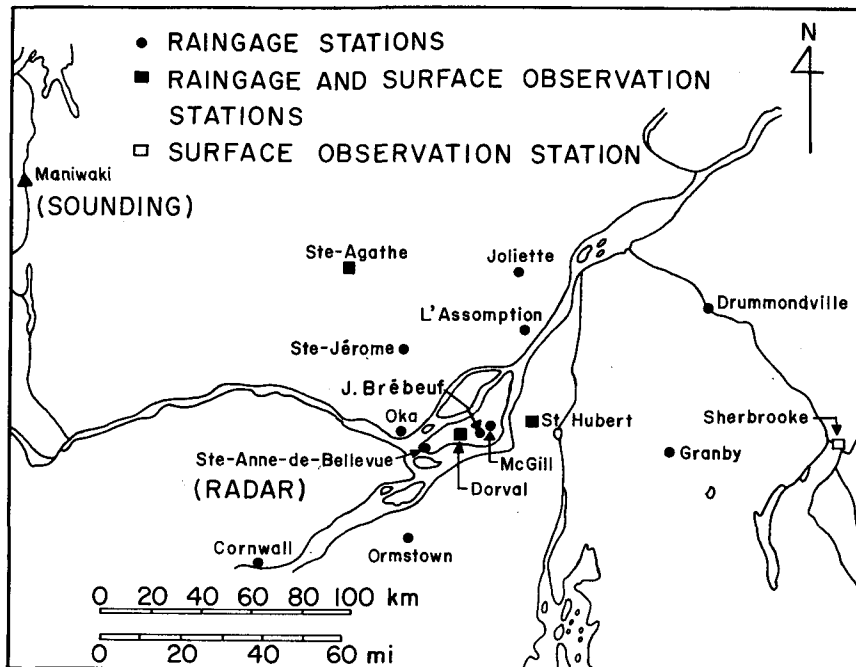


FIG. 1. Geographical distribution of the observation stations.

these maxima are not specified. However, the hourly amounts are also given so that by inspection of the radar maps and hourly amounts the times of occurrence of the rain rate maxima were determined. For moderate and high rates the hour of occurrence of the maximum rate is unambiguous. Light rain rates presented a problem in this respect and their time of occurrence is poorly determined.

Tipping-bucket gages measure very low rain rates poorly. Thus, 5 min maxima lower than 2.5 mm h^{-1} , that is, one tip of the bucket, cannot be measured. Consequently, cases with very low intensities were not considered in this study. The various sources of error of an operational tipping-bucket gage were studied by Weiss (1964). This study, as well as the experience with operational reading of chart records from gages by one of the authors, lead us to an estimation of an error of 20% for moderate and high 5 min rates, and smaller errors for rates over longer periods.

To obtain convective energies, the Maniwaki soundings, assumed representative of the Montreal area, were used. For each day two energies were calculated. For the first, the point with the highest value of the wet bulb potential temperature θ_w was selected from the sounding profile from the ground up to 600 mb (60 kPa). For the parcel defined by this point the positive area on the tephigram (from the lifting condensation level to the upper intersection of the pseudoadiabat and the sounding) was computed. Second, the energy was computed in the same way for the most energetic ground parcel defined by the highest value of θ_w selected from the 24 h readings of the four ground

stations. The procedure is illustrated in Fig. 2. Thus, for every day of the two seasons, the maximum energy was obtained for the convective parcels originating from instabilities in the sounding itself and for the convective parcels originating at the ground in the Montreal area.

The Montreal ground station was not considered for the surface data selection to avoid introducing extreme surface conditions in a study in which the precipitation was to be observed on an area much larger than the one over which the urban effect could be acting.

To decide which of the two daily soundings was to be used to calculate the daily maximum of the surface parcel convective energy the following criterion was used: for the 24 h period in which the maximum rainrate R_{\max} occurred the maximum value of θ_w was chosen from all the 24 hourly recordings of the four ground stations and this value was applied to the *immediately previous* sounding to determine the energy. This criterion for the calculation of the maximum energy is not the only reasonable one; others were also applied and will be discussed in Section 5. The one described here is the most adequate if we envision a possible application of the present work to the forecasting problem. The inconvenience of this particular criterion is that the energy maximum E_{\max} can occur and, in fact, it does so on some occasions, after the occurrence of the maximum rainfall rate. The authors accepted this possibility under the assumption that values close to R_{\max} and E_{\max} occur several times during the day and by increasing the sample size the chances of detecting

the maximum of energy increases. We do not claim that the parcel for which the energy was calculated produced the measured rain. It is by sampling in time and space that we detect the maximum convective energy for a particular meteorological situation and correlate that energy with the maximum intensity of precipitation which occurred under the given conditions. It is obvious that not all of the intense rain cells are detected by the gage network. In a multicell precipitation event the same R_{max} will be present at a few different times and places. We also verified the recurrence of values of energy very close to the daily maximum.

3. Results

During the two summer seasons 144 storm systems were detected by the gage network, with a storm system defined by precipitation with discontinuities shorter than 5 h as revealed by the gage network. That is, if over a period of 5 h not a single gage of the network reported precipitation, the next rain event was considered to be part of a new system. Of these systems 106 were well-documented by complete radar and rain-gage data. For these storms, the scattergram of Fig. 3a indicates, along the ordinate, the maximum rainfall rate R_{max} (measured over 10 min) as detected by the gages and, along the abscissa, the maximum energy E_{max} calculated as described in the previous section. The indicated energies correspond to either the surface parcel or the upper air parcel whichever energy was greater. The correlation between R_{max} and E_{max} as shown in Fig. 3a is very weak, with a correlation coefficient $\rho=0.49$.

We now proceed to filter the data as follows: With the aid of radar records we deleted the cases for which the most intense precipitation missed all of the 14 gages (41 cases). To determine this, radar maps at the same time as the hour of occurrence of the maximum rain rate were inspected. If the strongest radar echo passed directly over the gage reporting the maximum rain rate we considered this a hit. Otherwise it was a miss. With this use of raingage and radar records we get as close as it is possible to the maximum rain rate. In fact the actual maximum rain rate could have been even higher. The quantization of radar echoes in 10 dB steps and the height difference between the radar beam and the raingage makes it impossible to tell whether the core of precipitation was actually detected. For the 41 cases for which the core was missed by the gages, R_{max} as given by the network is obviously underestimated and we could expect that cases with small R_{max} for a given E_{max} fall into this group. By eliminating these cases from Fig. 3a, we obtain Fig. 3b, with a much improved correlation ($\rho=0.67$). Second, we consider the cases for which the energy of the upper air parcel is greater than the energy of the surface parcel (11 cases). For these, the energy is poorly sampled

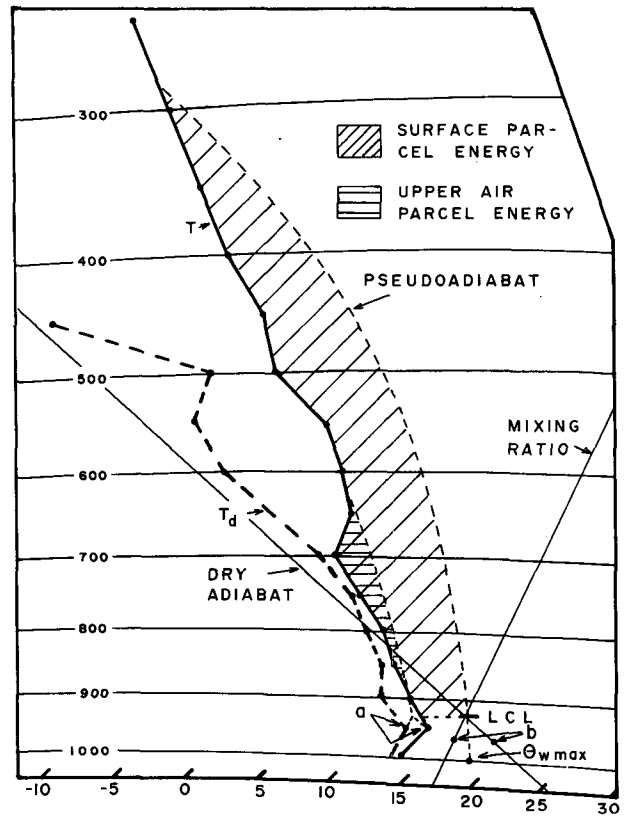


FIG. 2. Maniwaki sounding and Montreal area maximum surface conditions on the tephigram 25 August 1970. The temperature and dew point (a) indicated on the sounding correspond to the upper air parcel with the maximum value of θ_w . This parcel generates our upper air convective energy. The indicated surface temperature and dew point (b) correspond to the ground parcel with the maximum value of θ_w as reported by the four ground stations. This parcel generates our surface maximum energy.

(every 12 h) and therefore probably underestimated. Points with low E_{max} for a given R_{max} should fall into this class. By eliminating these from Fig. 3b, Fig. 3c is obtained. A clear correlation between E_{max} and R_{max} is now apparent, with a correlation coefficient $\rho=0.74$.

The filtering process leading from Figs. 3a to 3c was given in detail because its logic and effect are as convincing of the relationship between E_{max} and R_{max} as the scattergram of Fig. 3c. It points to the importance of the sampling problem, in energy and rain, for the determination of the relationship between E_{max} and R_{max} . In particular the radar data, although used qualitatively, were crucial. Without them it would not have been possible to go beyond Fig. 3a in spite of the relatively good standard observation raingage network available.

There are five cases in Fig. 3c with high rain rates which stand out from the rest. Not only were the rates high in these cases, they also were more persistent.

In Fig. 4, the 5 min maxima of rain rates are represented on the ordinate. The five points (circled) still have the highest rates, although they are not as clearly

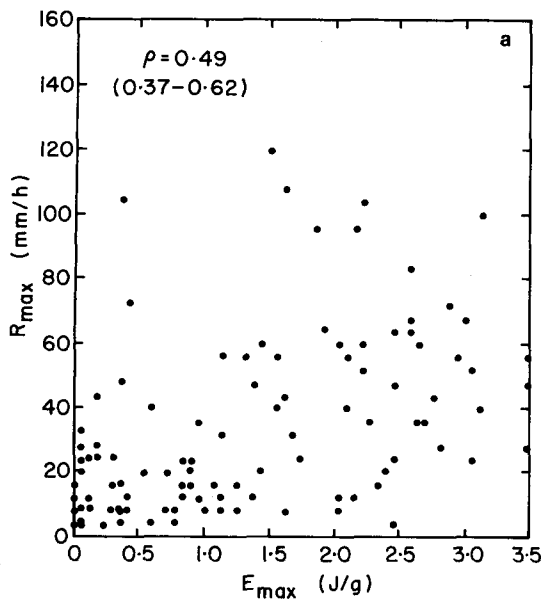


FIG. 3a. Scattergram of daily maximum rain rate (take over 10 min) versus daily maximum convective energy for the 106 cases for which complete records of precipitation and surface temperature and humidity were available. The values in parentheses are the confidence limits of ρ for a level of significance of 0.05.

separated from the rest of the points. The fact that they differentiate as we go from 5 to 10 min maxima of rain rates is an indication of the persistence of the high rates.

The numbers accompanying each point in Fig. 4 are the time differences in hours between the occurrence of R_{\max} and E_{\max} , that is, $\Delta t = t(R_{\max}) - t(E_{\max})$. These

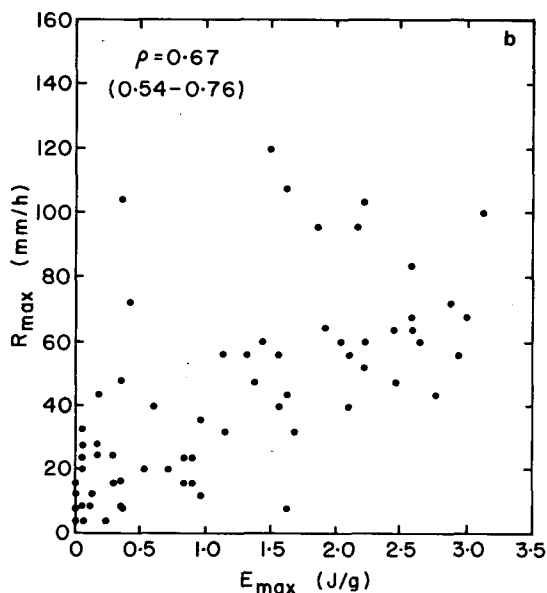


FIG. 3b. As in Fig. 3a except for the 65 cases in which the maximum rain rate was detected by one of the raingages.

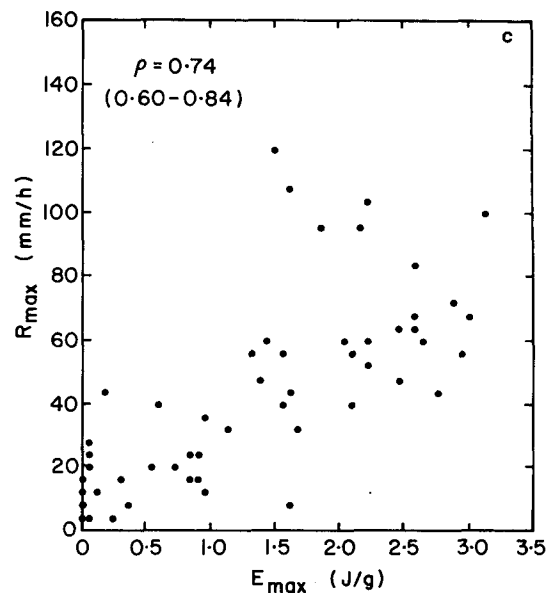


FIG. 3c. As in Fig. 3a except for the 54 cases for which the maximum rain rate was detected by the raingage network and the maximum of energy corresponded to the surface parcel.

time differences are known with a ± 1 h certainty for moderate and intense rain. The distribution of Δt is practically random with 25% of the cases falling between ± 1 h. It should be mentioned, however, that some of the values of Δt could be somewhat reduced without any appreciable change of points in Fig. 4 by choosing values of energy very similar to E_{\max} but closer in time to the occurrence of R_{\max} . The variability of the surface θ_w has a random component so that extreme values may appear several times during the day (at the same or another station) and this variability is reflected in the parcel energies. It is the belief of the authors that precisely this recurrence of extreme values of θ_w coupled with enough sampling is at the root of the success in establishing the correlation between E_{\max} and R_{\max} .

In Fig. 5, the best-fit linear regression lines are given for rain rate maxima taken over 5, 10, 15 and 30 min with the correlation coefficients indicated in brackets. It is seen that the shorter the averaging time the better is the correlation, indicating that, in effect, it is the *maximum* rain rate produced by a precipitation system which is determined by the maximum energy available.

Some of the scatter of points in Fig. 4 is due to measurement errors in R_{\max} and soundings as well as errors and scarcity of the surface data, but most of it is surely a consequence of the oversimplification implied by the parcel method. One obvious and important effect which affects precipitation is frontal lifting. It is expected that vertical motion on a synoptic scale could produce precipitation even in the absence of parcel convective energy. This would explain the fact that for $E_{\max} = 0$ the best-fit lines in Fig. 5 cross the vertical

axis at an appreciable value of R_{max} . Also frontal situations should have a more variable R_{max} depending on the strength of the uplifting and, on the average, higher rates of precipitation than for air mass cases.

By inspecting the weather maps (surface, 85 and 70 kPa) for the cases reported in Fig. 4, 15 events were found such that clearly no frontal passage occurred in our region within a 12 h period, or longer, around the time of R_{max} . These were considered as air mass cases. In Fig. 6 these 15 cases are shown with the best-fit line. The correlation coefficient is 0.89. The remaining departure from the origin can be attributed to the fact that our analysis is restricted to a positive quantity (rain rate). All the points in Fig. 6 are located at the lower boundary of the scattergram of Fig. 4. Although the sample size is small the results are highly significant not only because the correlation coefficient is high but also because all the expected differences between frontal and air mass cases are present.

The correlation coefficient between R_{max} and E_{max} for the 39 remaining cases is $\rho=0.80$, so that our division into frontal and air mass cases produces in effect two distinct populations each with a value of ρ higher than the ensemble.

4. Influence of upper air humidity

The results presented so far involved both parcel conditions and vertical temperature profiles, although the vertical distribution of humidity was not considered. However, through the entrainment mechanism or by frontal lifting the ambient humidity could play a substantial role in the production of rain. Consequently correlations were made between the mean humidity

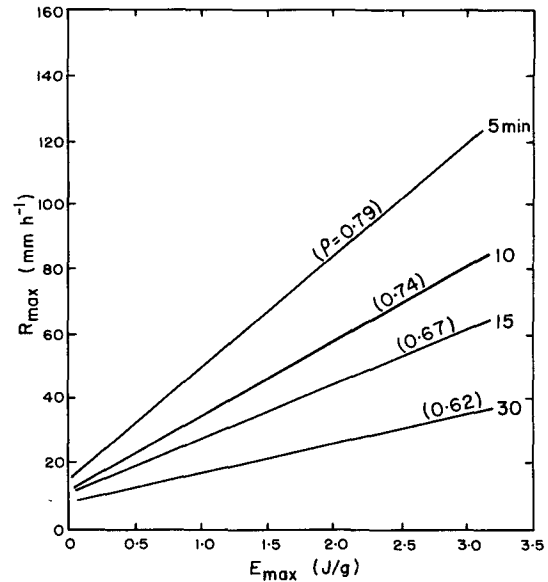


FIG. 5. Linear regression lines of R_{max} vs E_{max} for the indicated time periods over which the maximum rain rate was taken.

over various depths of the atmosphere above the 950 mb level (95 kPa) and maximum rain rate. Also, the influence of humidity at each level was studied. The moisture parameters considered were mixing ratio and relative humidity. Considering the mean humidity parameters over a variable depth, the results can be summarized as follows:

- 1) For all the 54 cases of Fig. 4 no significant corre-

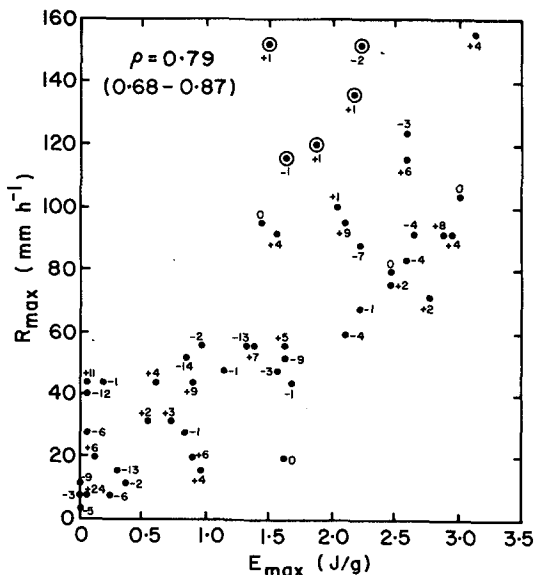


FIG. 4. Scattergram of 5 min maximum rates versus the maximum energy for the same cases as in Fig. 3c. The numbers accompanying each point are the time differences in hours between the occurrence of R_{max} and E_{max} .

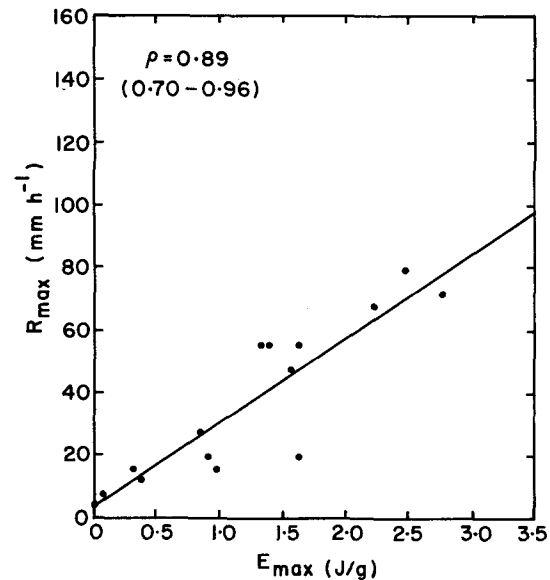


FIG. 6. Scattergram and best-fit line of daily 5 min maximum rain rate as a function of daily maximum surface convection energy for 15 air mass cases.

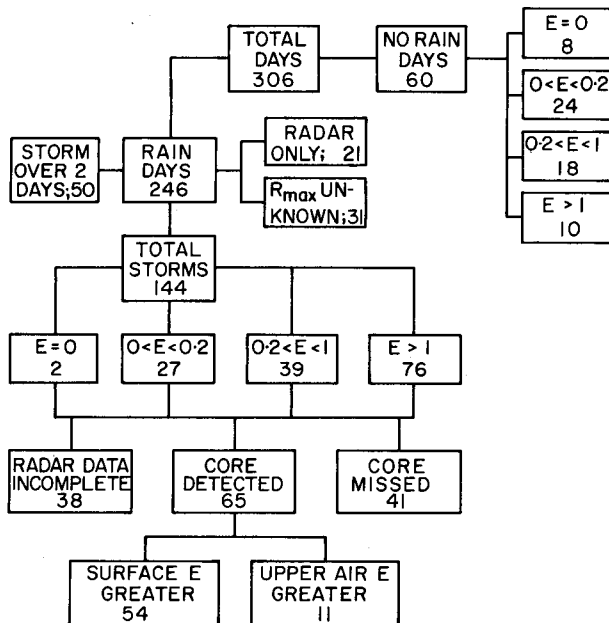


FIG. 7. The breakdown of the 306 days considered in this study.

lation was found between R_{\max} and the mean upper air relative humidity for any depth of the atmosphere.

2) Upper air mean mixing ratio, however, correlates with R_{\max} with a correlation coefficient of $\rho \approx 0.6$ with slight variations depending on the layer over which the mean is taken. The variation of ρ shows, nevertheless, a systematic decrease from $\rho = 0.61$ to $\rho = 0.54$ as the top of the layer increases from 800 mb to 500 mb and remains steady thereafter.

3) The multiple-correlation coefficient of R_{\max} with convective energy and the mean mixing ratio increases with increasing depth up to a maximum of $\rho = 0.82$ for the 950–600 mb layer and no further improvement is found when higher layers are considered. Energy and mean mixing ratio are weakly correlated ($\rho = 0.46$).

4) If only the 15 air mass cases are considered, the correlation between mean mixing ratio and R_{\max} drops to $\rho = 0.47$, with the top of the layer at 800 mb and decreasing with depth. No improvement in the correlation between energies and rain rates is obtained in these cases by introducing the upper air humidity; the multiple correlation coefficient remains $\rho = 0.89$.

When the humidity of each individual level was considered, the correlations, although somewhat improved, appeared to be showing only statistical fluctuations with no consistent behavior.

Although these results should be taken as indications for further research rather than conclusive in themselves, it seems that upper air humidity is important in determining the maximum rate of precipitation, particularly in the frontal cases. These results, however, should be considered with some caution since the upper

air humidity information is, in some cases, affected by radiosonde's penetration of clouds.

5. More results

a. A breakdown of cases

A rain day is defined by observation of precipitation by either the raingage network or by radar at an antenna elevation of 2° when the radar pattern was over the region covered by the gages. By this definition 246 calendar days out of the 306 comprising the two summer seasons, that is 80%, were rain days. This rain was produced by 144 storm systems, with storms system defined in Section 3.

There were 50 storms extending over two days. As indicated in Fig. 7, 21 days had incomplete raingage records and in 31 days the precipitation was too light to be measured precisely by tipping-bucket gages. Two of the 144 storms occurred while the calculated parcel energy was nil, i.e., in 1.4% of the cases. The radar data showed that out of the 144 storms, 65 had the most intense precipitation passing over one of our gages, while in 41 cases (28%) the core of precipitation was not detected by the network. In 38 cases the radar data were either incomplete or entirely missing and thus the detection of the maximum of precipitation by the gages was impossible to determine. The 65 plus 41 storms, for which we had complete data, were the subject of our study.

On the other hand, the 60 days with no detectable rain had a complete distribution of convective energies. In our method of energy calculation no distinction is made between instability and latent instability. Neither is there taken into account the possibility of synoptic-scale subsidence or the change in upper air conditions between the time of the sounding and the occurrence of the maximum surface conditions. Particularly disturbing are the 10 days with energies greater than 1 J/g^{-1} , for which the possibility of obtaining energies caused by measurement errors is negligible. The authors felt that it was preferable to keep the method of analysis simple even at the cost of failing to predict no-rain days. Therefore, the results described in the previous sections should be taken as conditioned to the occurrence of rain. That is, if rain occurs, the maximum parcel convective energy is related to the maximum of rain rate as described in Sections 3 and 4.

b. Influence of surface conditions

One immediate question which comes to mind in relation to the correlations described in the previous sections is how much of the relationship between R_{\max} and E_{\max} is determined by the values of surface maximum θ_w , i.e., $\theta_{w \max}$, and how much of it is the influence of the upper air conditions. To answer this question a correlation was made between $\theta_{w \max}$ and R_{\max} for the same storms as in Fig. 4. The correlation coefficient is

as high as $\rho=0.75$ for the 5 min rain rate maxima and $\rho=0.69$ for the 10 min R_{\max} (as compared to 0.79 and 0.74 for Fig. 4 and Fig. 3c, respectively). Thus $\theta_{w \max}$ determines quite well the maximum rate of precipitation. This result is not surprising since energy is quite sensitive to θ_w which in turn has an appreciably greater variability than the upper air conditions.

However, energies are preferable to θ_w in the attempt to establish a relation with precipitation since, beyond a higher value of ρ , they offer many possibilities of improvement in the correlation. For example, when a correlation is made between $\theta_{w \max}$ and 5 min R_{\max} for the air mass cases, the correlation coefficient remains $\rho=0.75$, while a significant improvement was obtained with energies. Even more significant is the fact that, when the upper air humidity is introduced with θ_w as has been done with E in Section 4, no improvement is obtained in the correlation between $\theta_{w \max}$ and R_{\max} .

c. Maximum rainfall from parcel theory

Standard textbooks give expressions to calculate the maximum rainfall rate for a given sounding based on the pseudoadiabatic parcel theory (see, e.g., Iribarne and Godson, 1973). One such expression is

$$R_{\max} = 3600 \frac{c_p}{g} \int \left(\frac{\Gamma_d - \Gamma_s}{L_v} \right) W dp, \quad (1)$$

where c_p is the specific heat at constant pressure, g the acceleration of gravity, Γ_d and Γ_s the adiabatic dry and saturated lapse rates, respectively, L_v the latent heat of condensation and W the vertical velocity. With W calculated by the parcel method, (1) was used to obtain R_{\max} for all the cases reported in Fig. 4 and the results were correlated with the actual 5 min maxima of rain rate. The correlation coefficient was $\rho=0.75$, a value somewhat lower than the one obtained with energies. The actual values of R_{\max} obtained from (1) were about 10 times greater than those measured by the gages.

d. Cloud tops from parcel theory

Cloud heights obtained from IR satellite imagery were used by Scofield and Oliver (1977) to estimate rainfall. Since parcel convective energies depend strongly on the height of convection, correlations were made between cloud-top heights obtained by the parcel method and the maximum rate of precipitation. For the 54 cases of Fig. 4 the relationship between the cloud-top heights H and 5 min R_{\max} was found to be

$$R_{\max} = 8 \exp(0.2H),$$

when R_{\max} is measured in millimeters per hour and H in kilometers. This relationship applies to values of $H > 1.5$ km. Only one case had H below this value. The linear correlation coefficient between $\ln(R_{\max})$ and H is $\rho=0.76$.

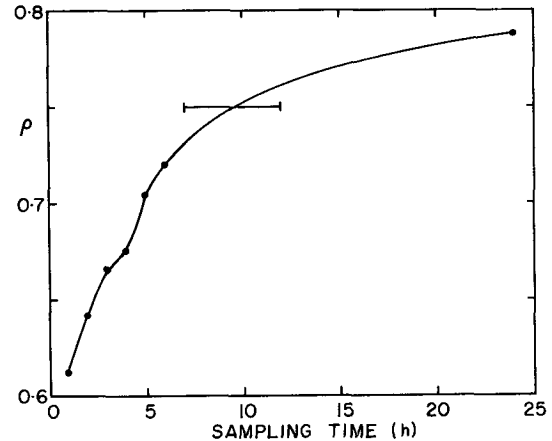


FIG. 8. Dependence of the correlation coefficient with the number of hours over which the maxima of surface conditions were sampled. The horizontal bar corresponds to a sampling time variable from 7 to 12 h (see text).

With the reservation concerning the parcel method's ability to determine cloud top heights, this could be a useful result for extending the meteorological use of satellites.

e. Alternative criteria for determining E_{\max}

The absence of relationship between the time of occurrence of E_{\max} and that of R_{\max} , mentioned in Section 3, could be particularly disturbing. Consequently, two alternative ways of selecting the maximum energy were implemented. Both imply a reduction in the sample size of E but a more logical sequence of events. In the first, the maximum value of the surface θ_w within a period of time varying between 1 and 6 h prior to the occurrence of R_{\max} was selected and applied to the immediately preceding sounding. The correlation coefficient between the maximum energies obtained in this way and R_{\max} increased steadily from $\rho=0.61$ to $\rho=0.72$ as the time over which the energy was sampled increased from 1 to 6 h.

In the second method $\theta_{w \max}$ was chosen from values occurring in the time interval going from the occurrence of R_{\max} back up to 6 h before the storm's first detection by the gages. The sampling time of energy varies in this case from storm to storm from 7 to 12 h, depending on how late in the storm's life the maximum rate occurred. The correlation coefficient between R_{\max} and E_{\max} , in this case, is $\rho=0.75$. Extending the sampling time up to 12 h for all the storms did not change the value of ρ .

In Fig. 8 the variation of ρ with the sampling time of energy values as given by the three methods of selection of E_{\max} is shown. The last point of the curve corresponds to the criterion for the selection of E_{\max} described in Section 2 and, therefore, is the only point for which the energy was sampled before and after the time of R_{\max} . It is seen that the correlation between

R_{\max} and E_{\max} increases with increasing sample time reaching a limiting value close to $\rho=0.8$.

It was not possible to determine if increasing the sampling in space could reduce the necessary sampling in time. In our case, two of the ground stations (Dorval and St-Hubert) provided most of the values of $\theta_{w \max}$ used to calculate E_{\max} .

In any case, the results summarized in Fig. 8 indicate that the hypothesis advanced in Section 3, namely, that the recurrence of values of θ_w close to $\theta_{w \max}$ and the importance of sampling, are responsible for the success in establishing the correlation between E_{\max} and R_{\max} .

6. Discussion and conclusions

The relationship between convective energies calculated by the parcel method and the maximum rate of precipitation has been established here with a high level of significance. The poorest correlation, that of E_{\max} and 30 min R_{\max} with $\rho=0.62$, has a level of significance better than 0.005.

The humidity in the upper levels plays an appreciable but secondary role in determining R_{\max} . The simplest hypothesis which accounts for these facts is that parcel convection originating at the surface is the main mechanism by which the extreme rain rates are produced in both frontal and air mass situations. However, the lack of relationship between the time of occurrence of E_{\max} and R_{\max} puts this hypothesis under question. The results discussed in Section 5e were intended to meet this objection, but only some well-documented case studies could definitely clarify this point. This is an important question since the role of the surface convection, coupled with the variability and recurrence of surface conditions, could be a triggering action by which most of the energy on a large-scale is concentrated and released in the small areas occupied by the convective elements.

The various correlation coefficients obtained by different combinations of the parameters considered in this work are of high statistical significance. The difference between these coefficients, however, are statistically marginal. As can be seen from the values given in each scattergram the confidence limits of all the obtained values of ρ overlap, so that many of the results presented here are tentative and must be verified with larger sample sizes and independent sets of data. However, the authors would like to put the

emphasis on the findings which, beyond statistical considerations, show a systematic consistency with physical intuition such as the various differences found between air mass and frontal cases described in the second half of Section 3.

The fact that the correlation between R_{\max} and E_{\max} is so high and is not dependent on the detection of unique values of surface and upper air conditions (standard network observations were used here) opens the possibility to practical applications of this work to the backcasting, and perhaps forecasting, of the maximum rate of precipitation for a given synoptic situation. A relationship between E_{\max} and R_{\max} could therefore be helpful in assessing the effectiveness of weather modification projects. Another area of application could be in parameterization of rain in convective models where the three-dimensional aspects of convection must often be left aside to permit the introduction of cloud microphysics.

Acknowledgments. Financial support for this work was provided by the National Research Council of Canada and the Ministry of Education of Quebec through its F.C.A.C. program.

The presentation of this work was improved, thanks to the comments of Drs. R. R. Rogers and G. Drufuca as well as those made by the reviewers.

REFERENCES

- Austin, P. M. and R. A. Houze, 1972: Analysis of the structure of precipitation patterns in New England. *J. Appl. Meteor.*, **11**, 926-935.
- Drufuca, G., 1977: Radar derived statistics on the structure of precipitation patterns. *J. Appl. Meteor.*, **16**, 1029-1035.
- , and I. I. Zawadzki, 1975: Statistics of raingage data. *J. Appl. Meteor.*, **14**, 1419-1429.
- Hamilton, 1966: Vertical profiles in shower situations. *Quart. J. Roy. Meteor. Soc.*, **92**, 346-362.
- Harnack, R. R., and H. E. Landsberg, 1975: Selected cases of convective precipitation caused by the metropolitan area of Washington, DC, *J. Appl. Meteor.*, **14**, 1050-1060.
- Huff, F. A., and W. L. Ship, 1969: Spacial correlations of storm, monthly and seasonal precipitation. *J. Appl. Meteor.*, **8**, 542-550.
- Iribarne, J. V., and W. L. Godson, 1973: *Atmospheric Thermodynamics*. D. Reidel, 222 pp.
- Scofield, R. A., and V. J. Oliver, 1977: A scheme for estimating convective rainfall from satellite imagery. NOAA Tech. Memo. NESS 86, Washington, DC, 47 pp.
- Weiss, M., 1964: The distribution of rainfall with rate at McGill Observatory. M. S. thesis, McGill University, 113 pp.